Noname manuscript No.
(will be inserted by the editor)

Statistical Spherical Wavelet Moments for Content-based 3D Model Retrieval

Hamid Laga[1], **Masayuki Nakajima**[2⋆]

[1] Global Edge Institute, Tokyo Institute of Technology e-mail: hamid@img.cs.titech.ac.jp
[2] Computer Science Department, Tokyo Institute of Technology e-mail: nakjajima@img.cs.titech.ac.jp

Received: date / Revised version: date

Abstract The description of 3D shapes with features that are invariant under similarity transformations is one of the challenging issues in content-based 3D model retrieval. In this paper we show that shape sampling affects significantly the rotation invariance of existing shape descriptors. Then we propose a new parameterization method that samples uniformly the shape which is then fed to a spherical wavelet analyzer to extract discriminative features. We introduce new shape descriptors based on higher order statistical moments of the spherical wavelet sub-bands of the spherical shape function. The proposed descriptors are compact and invariant under similarity transformations. We demonstrate their efficiency, using the Princeton Shape Benchmark, regarding the computational aspects and retrieval performance.

Key words 3D retrieval spherical wavelets moments shape parameterization rotation invariance.

1 Introduction

Recent advances in 3D acquisition and modeling techniques have stimulated the use of 3D data in various fields, resulting in the accumulation of 3D models in large data sets. As 3D data are becoming widely spread and ubiquitous, the need for tools for their efficient storage and retrieval is significantly increasing. In contrast to text and text-based retrieval, content-based retrieval of 3D models (CB3DR) from large databases implies the use of geometric shape features for indexing the data. A challenging issue is the description of shapes with suitable numerical representations called *shape descriptors*.

In general a shape descriptor should be discriminative by capturing only the salient features, robust to noise, compact, easy to compute, and invariant under similarity transformations such as translation, scale and rotation [16, 12, 25]. Other invariant properties may be required for some applications, such as pose invariance for matching articulated shapes [7, 23].

In this paper, we demonstrate that shape sampling methods, we call *parameterization*, affect significantly both the rotation invariance and the retrieval performance. We introduce a new parameterization method that is fully rotation invariant, and therefore the rotation invariance of the descriptor will depend only on the sampling resolution. Then we propose new shape descriptors that are based on spherical wavelet coefficients, and higher order statistical moments of the wavelet sub-bands.

This paper is organized as follows. In the next section we review the related work and outline our contributions. Section 3 discusses the limitation of existing shape parameterization methods and describes our method that is invariant to rotation. Section 4 reviews the general concepts of spherical wavelet analysis of functions defined on the sphere, and describes how we use them for 3D shape analysis. Section 5 describes in detail the proposed shape descriptors. Section 6 presents some experimental results. Finally, we discuss the obtained results and point further directions of this research.

2 Related work

Most of three-dimensional shape retrieval techniques proposed in the literature aim to extract from the 3D model meaningful descriptors based on the geometric and topological characteristics of the object. Survey papers to the related literature have been provided by Tangelder et al. [24] and Iyer et al. [9]. In the following, we review the most efficient shape descriptors as well as existing methods for extracting rotation invariant features.

2.1 Shape descriptors

Descriptors are used to compare 3D models. Existing techniques can be classified into three broad categories; feature-based including global and local features, graph-based and view-based similarity.

⋆ *Present address:* I2-12-1,S6-9, Ookayama, Meguro-ku, Tokyo 152-8552

View-based techniques compare 3D objects by comparing their two dimensional projections. They are suitable for implementing query interfaces using sketches [9,6]. The Light-fields (LFD) [2] are reported to be the most effective descriptor [22]. LFD are shape features computed from 2D views taken from view points uniformly distributed on the geodesic sphere. This allows to account equally for all shape features and are rotation invariant. However, they are very expensive in terms of computation power (descriptor computation and comparison) and storage. We overcome this limitation by using spherical wavelet descriptors.

Graph-based techniques compare 3D shapes by comparing their two dimensional descriptors. Reeb graphes [7], and skeletons [23] are among the most popular. Cornea et al. [3] used the skeletal representation of 3D volumetric objects for many-to-many and part matching.

Feature-based methods aim to extract compact descriptors from the 3D object. Johnson et al. [10] introduced spin images as local features for matching 3D shapes. They have been used for shape retrieval as well as for the matching and registration of 3D scans. Other techniques are based on the distribution of features, such as shape distributions [15]. Shilane et al. [22] provided a comparison of these techniques and reported that histogram-based methods are the less efficient in terms of discriminative power.

Recently, Reuter et al. [18] introduced the notion of shape DNA. They proposed fingerprints for shape matching. The fingerprints are computed from the spectra of the Laplace-Beltrami operators. These descriptors are invariant under similarity transformations, and are very efficient in matching 2D and 3D manifold shapes. However, it is not clear how they can be extended to polygon soup models. Our proposed technique applies on polygon soup models without any restriction on the topology of the shape.

2.2 Invariant features

The issue of extracting invariant shape features is an important problem in content-based 3D model retrieval. While translation and scale invariance can be easily achieved [20,6,12], rotation invariance is still a challenging issue. Various methods have been proposed to cope with the problem. Some of them require pose normalization, where each shape is placed into a canonical coordinate frame. These methods are based on the Principal Component Analysis (PCA) [11], and continuous PCA [26], with extensions for solving for axial ambiguity. However, PCA-based alignment is known to misbehave and therefore, it hampers significantly the retrieval performance [12].

To avoid explicit alignment, the shapes are represented using functions defined on the unit sphere. Funckhouser et al. [6] uses spherical harmonics (SH) to analyze the shape function. Spherical harmonics can achieve rotation invariance by taking only the power spectrum of the harmonic representation, and therefore, discarding the rotation dependent information [12]. Novotni et al. [14] uses 3D Zernike moments

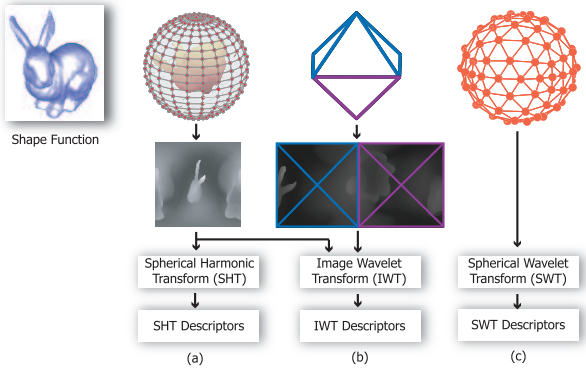

Fig. 1 Illustration of different parameterization methods; (a) two singularities; one at each pole. (b) The singularities are eliminated but the sampling is not uniform near the six vertices of the octahedron. (c) Uniform sampling.

(ZD) as a natural extension of SH. Representing 3D shapes as functions on concentric spheres has been extensively used. Our developed descriptors fall into this category and are a natural extension of SH and ZD.

Laga et al. [13] uses flat octahedron parameterization and wavelet descriptors. This eliminates the singularities that appear in the two poles when using latitude-longitude parameterization but it introduces singularities near the six vertices of the octahedron. Moreover, image wavelets respond to horizontal and vertical features, and therefore, they are sensitive to rotations of the spherical function. We overcome this limitation by using the second generation wavelets and augment the energy descriptors with higher order statistical moments of the wavelet sub-bands to capture more features of the shape.

3 Rotation invariant parameterization

Unlike 2D images, 3D models lack proper parameterization. When dealing with watertight meshes with low genus, geometry images and spherical parameterization have been introduced in the context of texture mapping and geometry compression [19,8]. The parameterization in this case is one-to-one. In the context of 3D model retrieval, however, most of the data are polygon soup models with arbitrary genus and without restriction on the topology. Luckily 3D retrieval does not require a one-to-one mapping but rather a parameterization that preserves the salient features of the shape. As illustrated in Figure 1, we consider three parameterization methods: (1) latitude-longitude parameterization, (2) octahedron parameterization and (3) uniform parameterization using geodesic sphere. The first one has been extensively used in the literature and, as shown in Figure 1-a affects the rotation invariance since it has singularities near the two poles. We discuss the two others in the following subsections.

3.1 Octahedron parameterization

Hoppe et al. [8,17] maps the sphere onto a rectangular domain using spherical parameterization of a *flattened octahedron*. The interesting property is that the flattened octahedron unfolds isometrically onto a rectangular lattice. Therefore, image processing tools can be used with simple boundary extension rules. This has been used in [13] for shape retrieval, as shown in Figure 1-b, and demonstrated that it can be used to reduce the singularities and therefore the sensitivity to rotations. However, this sampling is not uniform since the distance between neighbor points is smaller near the six vertices of the octahedron.

3.2 Uniform parameterization using geodesic dome

The key idea of our approach is that rotation invariant sampling can be achieved using an operator Φ that samples the shape uniformly, in the Euclidean distance sense, in all directions.
To achieve this in practice, we sample the shape function by casting rays from the shape's center of mass to the vertices of a geodesic dome. Figure 1-c illustrates this principle. The advantages of this representation are two fold; first the vertices of the geodesic dome are equidistant, all its faces are of equal area, and is free of any singularity. Therefore, it guarantees a uniform sampling of the shape. Second, it allows a multiresolution analysis of the shape function where the coarsest (level-0) representation is obtained using a basic octahedron of 20 vertices, and finer levels are derived by recursive subdivisions.

4 Wavelet analysis for 3D shape description

Discriminative feature extraction is much easier if it is done via transformation of the shape function, we computed in the previous section, into a suitable space where simple models with small number of parameters can describe the data. Since at this stage our shape function is defined as an image on the spherical domain, we import some ideas from texture analysis. Particularly, we first apply a wavelet transform to the spherical shape signal, using either image wavelets or spherical wavelets. The resulting sub-bands are then run through a statistical analyzer module to build discriminative shape descriptors.

For the wavelet analysis stage, we present two alternatives following the work of Hoppe et al. [8] on shape compression, that we adapt to our purpose.

4.1 Image wavelets with spherical boundary extension (IWT)

Similar to [8], all what we need is to set the boundary extension rules then use standard image wavelet packages for analyzing the shape function.

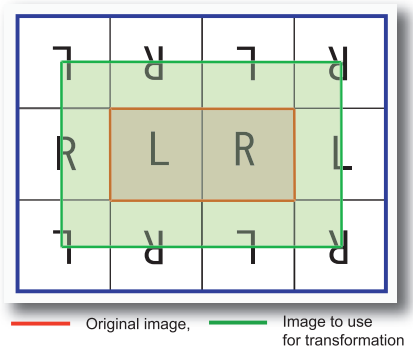

Fig. 2 Implementation of the boundary extension for image wavelet transform (IWT). The orientation of the letters indicates the way the image halves are flipped.

The image wavelet transform (IWT) uses separable filters, so at each step it produces an approximation image A and three detail images HL, LH, and HH. The forward transformation algorithm performs as follows:

1. **Initialization:**
   (a) Generate the geometry image I (therefore the function f) of size $w \times h = 2^{n+1} \times 2^n$ using octahedron parameterization as explained in Section 3.1.
   (b) $A^{(n)} \leftarrow f$, $l \leftarrow n$.
2. **Forward transform:** repeat the following steps until $l = 0$:
   (a) Apply the forward spherical wavelet transform on $A^{(l)}$, we get the approximation $A^{(l-1)}$, and the detail coefficients $C^{(l-1)} = \{LH^{(l-1)}, HL^{(l-1)}, HH^{(l-1)}\}$ of size $2^l \times 2^{l-1}$.
   (b) $l \leftarrow l-1$.
3. **Collect the coefficients:** the approximation $A^{(0)}$ and the coefficients $C^{(0)}, \ldots, C^{(n-1)}$ are collected into a vector F.

We experimented with Haar and Daubechies bases but found that they provide similar retrieval performance. In this paper, we use the Haar wavelets which are easy to implement. In Haar wavelets, the scaling function is designed to take the rolling average of the data, and the wavelet function is designed to take the difference between every two samples in the signal.

The boundary extension rules During the wavelet transform, when processing a point that is closer to the image boundary than the wavelet kernel width, points outside the image boundary are invoked. The boundary extension rules come into play in such situations. For image wavelet transform, we apply very simple tricks. We first extend the image size by flipping the left and right halves of the image as shown in Figure 2. In this figure, the original image is delimited with a red boundary. The boundary is extended to the blue borders. We then analyze the entire extended image with an ordinary image wavelets. Finally we collect only the wavelet coefficients which are inside the green boundary. This procedure is very simple to implement, but it requires more memory stor-

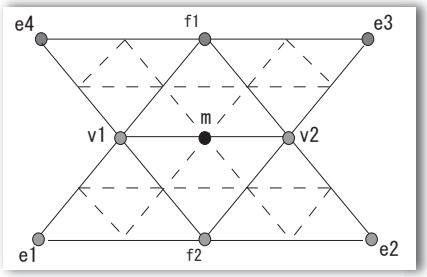

Analysis

$\forall k \in K(j)$: $A_{j,k} = A_{j+1,k}$

$\forall m \in M(j)$: $C_{j,m} = A_{j+1,m} - \sum_{k \in K_m} \tilde{s}_{j,k,m} A_{j,k}$

$\tilde{s}_{v_1} = \tilde{s}_{v_2} = 1/2,$

$\tilde{s}_{f_1} = \tilde{s}_{f_2} = 1/8,$

$\tilde{s}_{v_1} = \tilde{s}_e = -1/16.$

Fig. 3 Spherical wavelet stencil (top) and the analysis algorithm. Here $K(j+1) = K(j) \cup M(j)$.

age and processing time. Nevertheless, we found that still it provides a processing time that is acceptable for retrieval.

4.2 Second generation wavelets (SWT)

This is based on spherical wavelets introduced by Schröder and Sweldens [21]; the unit sphere is sampled at different resolutions. The base (coarsest) sampling level is an octahedron, and finer levels are obtained progressively by applying subdivision rules such as Loop or Butterfly. In our implementation, we used FSW (Fast Spherical Wavelet) package provided by Gabriel Peyre [1].

Figure 3 illustrates the forward analysis at each level j, $j = 0,\ldots,n-1\}$. Similar to IWT, we collect the approximation coefficients A^0 and the details coefficients at each sub-band C^j into a vector F, of length $2+4^{n+1}$, which we will use for descriptor extraction. Note that, we are only interested in the analysis step. For more mathematical details, we refer the reader to the original paper [21]. This scheme is very interesting to consider. In fact the analysis is not restricted to horizontal and vertical directions, as in image wavelet, but consider the one-ring neighborhood. Therefore, the analysis is less sensitive to rotations.

5 Wavelet-based descriptors

For the two parameterization methods we build two types of descriptors: one using a subset of the wavelet coefficients and the other based on wavelet moments.

5.1 Wavelet coefficients as shape descriptor

Once the spherical wavelet transform is performed, one may use the absolute value of the wavelet coefficients as a shape descriptor. Using the entire coefficients is computationally expensive. Instead, we have chosen to keep the coefficients up to level d. This is reasonable since many of the high frequency coefficients are either noise components or null in case of smooth geometry images. We call the obtained descriptors IWT_COEFFS and SWT_COEFFS for, respectively, image wavelet transform and spherical wavelet transform, where $d \in \{0,\ldots,n-1\}$. In our implementation we used $d = 3$, therefore, the IWT_COEFFS descriptor is of size $N = 2^{d+2} \times 2^{d+1} = 32 \times 16$, and the SWT_COEFFS is of size $N = 258$.

Comparing directly wavelet coefficients requires efficient alignment of the 3D model prior to wavelet transform. We perform a PCA-based pose normalization [16] and compute the Euclidean distance as a dissimilarity measure between two feature vectors F_1 and F_2. Note that, the vector F provides an embedded multi-resolution representation of the 3D shape features. This approach performs as a filtering by removing outliers. A major difference with spherical harmonics is that IWT and SWT preserve the localization and orientation of local features.

5.2 Wavelet moments

Traditional approaches computed energies of the wavelet subbands as features. They have been used in texture description for image retrieval [27,4,5], and later for 3D model retrieval [13]. Commonly, L^1 and L^2 norms are used as measures.

A natural extension of the energy method is to treat the wavelet sub-band analysis as a probability inference problem. We model the shape function by the marginal probability distribution of its wavelet sub-band coefficients. In this work, considering complexity as a major concern in 3D model retrieval, we simply characterize the wavelet sub-bands with their statistical moments.

The maximum likelihood (ML) estimator of the first moment is given by the sample mean:

$$F_l^{(1)} = \frac{1}{k_l} \sum_{j=1}^{k_l} |x_{l,j}| \tag{1}$$

where $\{x_{l,j}, j = 1 \ldots k_l\}$ are the wavelet coefficients of the l^{th} wavelet sub-band, and k_l is the number of coefficients in the $l-th$ wavelet sub-band. The first moment provides a summary of the information contained in each wavelet subband, and thus, it is a potential candidate for shape description. However, similar to the power spectrum [12], information such as feature localization are lost. To include more invariant properties in the shape descriptor we use higher order statistical moments. For instance, the second and third moments about the mean (standard deviation and skewness) are given by the following unbiased estimators:

$$F_l^{(2)} = \left(\frac{1}{k_l - 1} \sum_{j=1}^{k_l} (|x_{l,j}| - \overline{x_l})^2 \right)^{1/2} \tag{2}$$

$$F_l^{(3)} = \frac{k_l\sqrt{k_l-1}}{k_l-2}\frac{\sum_{j=1}^{k_l}\left(\left|x_{l,j}\right|-\overline{x_l}\right)^3}{\left(\sum_{j=1}^{k_l}\left(\left|x_{l,j}\right|-\overline{x_l}\right)^2\right)^{3/2}} \quad (3)$$

where $\overline{x_l} = F_l^{(1)}$ is given by Equation 1. To build the shape descriptor we first compute the three moments of the approximation $A^{(1)}$ and the moments of each detail sub-band yielding into a one-dimensional shape descriptor $F = \{F_l\}, l = 0 \ldots N$ of size $N = (3 \times (n-1)+1) \times 3$ for IWT descriptors, and $3 \times n$ for SWT descriptors. In our case we use $n = 7$, therefore $N = 19 \times 3$ for the IWT descriptor, and $N = 7 \times 3$ for SWT descriptor.

Observe that rotating a spherical function does not change its moments. Therefore, spherical wavelet moment-based descriptors are invariant under any rotation. Since the sampling stage is also rotation invariant, we obtain shape descriptors that are invariant to general rotations. Moreover, the moment descriptor is very compact. Thus, the storage and computation time required for comparison are reduced. Table 1 summarizes the length of the proposed descriptors for each parameterization method. Their discrimination efficiency and retrieval performance will be discussed in the experimental results section.

6 Experimental results

We have implemented the algorithms described in this paper and evaluated their performance on the Princeton Shape Benchmark (PSB)[22]. SWT_COEFFS and IWT_COEFFS require pose normalization while the moment descriptors are rotation invariant. To evaluate the efficiency of the proposed descriptors for shape retrieval we use the *Spherical Extent Function*(EXT) [20]; this is a measure of the extent of the shape in the radial direction. Note that our framework applies for any other spherical function such as the Gaussian Euclidean Distance Transform (GEDT) [12]. We chose to use the spherical extent function for its simplicity.

Comparing shape descriptors requires the definition of a distance metric in the feature space. We have experimented with the City block distance, the Euclidean distance and the Canberra metric and found that the Canberra metric achieves slightly better performance compared to the other two measures. Therefore, all the results we show in the following subsections are based on this metric. Recall that the Canberra metric between two vectors $X = (x_1, \ldots, x_n)$ and $Y = (y_1, \ldots, y_n)$ is defined as follows:

$$\mathscr{D}(X,Y) = \frac{1}{n}\sum_{i=1}^{n}\frac{|x_i - y_i|}{|x_i| + |y_i|}. \quad (4)$$

6.1 Retrieval performance

The precision-recall curves on the base test classifications of the PSB of the spherical wavelet-based shape descriptors are shown in Figure 4. We refer the reader to the Princeton Shape Benchmark paper [22] for comparison with other descriptors on the precision-recall measure.

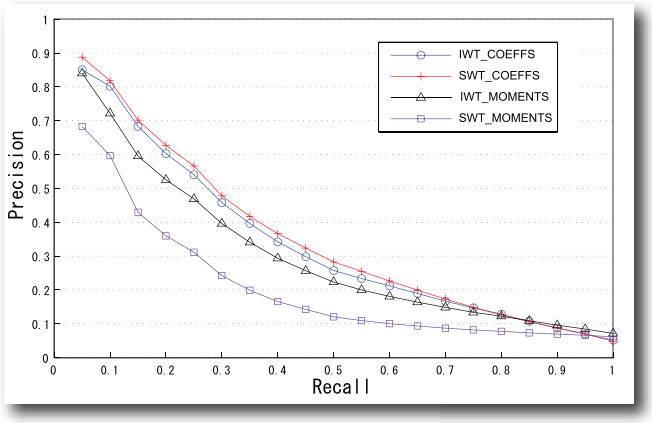

Fig. 4 Precision-recall graph for the four descriptors when using the base test classification of the Princeton Shape Benchmark.

We also evaluated the performance of our descriptors using the nearest neighbor, first and second-tier, E-measure and Discount Cumulative Gain measures [22]. The results are summarized in Table 1. We made all the experiments on the base test classification of the PSB. Table 1 shows that the spherical wavelet coefficients perform better, while the moments come in the second. Note that the wavelet coefficients require more storage and comparison time.

Shilane et al. [22] summarized the performance on the PSB of several shape descriptors and we use their results to compare with our descriptors. In this paper, we show the performance of six descriptors, but we refer the reader to the original paper for a complete evaluation. More precisely, we consider the:

1. **Lightfields descriptors (LFD) [2]**: they are computed from 100 images, which are rendered from cameras positioned on the vertices of a regular dodecahedron. Each image is encoded with 35 Zernike moments, and 10 Fourier coefficients. The dimension of the feature space is 4500.
2. **Gaussian Euclidean Distance Transform (GEDT) [12]**: Each spherical shell of the GEDT is represented by its spherical harmonic coefficients up to order 16 [12,22]. It uses the latitude-longitude parameterization.
3. **Spherical Harmonic Descriptor (SHD) [12]**: a rotation invariant representation of the GEDT obtained by computing the restriction of the function to concentric spheres and storing the norm of each harmonic [12,22].
4. **Spherical Extent Function (EXT) [20]:** It was computed on 64×64 spherical grid using the latitude-longitude parameterization and then represented by its harmonic coefficients up to order 16. We obtain feature vectors of 153 floating point numbers.
5. **Harmonics of the Spherical Extent Function (H-EXT) [12]:** a rotation invariant representation of the EXT obtained by computing the norm of each harmonic. In our implementation, we consider the harmonic coefficients up

Table 1 Retrieval performance of the wavelet-based descriptors, micro-averaged over all the models. We use the base test classification of the Princeton Shape Benchmark.

	Size	Nearest Neighbor	First tier	Second tier	E-measure	DCG
IWT_COEFFS	512	44.98%	32.00%	40.60%	21.22%	65.58%
SWT_COEFS	258	45.75%	33.61%	41.82%	22.65%	66.00%
IWT_MOMENTS	57	33.18%	28.6%	40.1%	21.41%	62.54%
SWT_MOMENTS	21	15.2%	19.7%	28.0%	14.34%	54.39%
LFD	4500	65.7%	38.0%	48.7%	28.0%	64.3%
SHD	544	55.6%	30.9%	41.1%	24.1%	58.4%
GEDT	4896	60.3%	31.3%	40.7%	23.7%	58.4%
EXT	153	54.9%	28.6%	37.9%	21.9%	56.2%
H-EXT	33	28.1%	24.5%	31.3%	16.3%	58.6%
D2	64	31.1%	15.8%	23.5%	13.9%	43.4%

to order 32 obtaining feature vectors of 33 floating point numbers. We used geometry images of size 128×128.

6. **Osada's** *D*2 **shape distribution (D2) [15]**: a one dimensional histogram that measures the distribution of the pairwise distance between pairs of random points on the shape surface. We used histograms of 64 bins.

In the literature, the LFD is considered as the best descriptor. Table 1 shows the results according to the quantitative measures computed on these descriptors (the results of LFD, EXT and D2 are the one reported in the original paper [22], while the results of H-EXT are from our implementation).

These results indicate that, spherical wavelet descriptors perform better than the LFD, shape distributions and spherical harmonic descriptors on DCG measure. An interesting observation is that the lightfield descriptor, which is considered a very good signature [2], performs better than spherical wavelet descriptors for the $k-$nearest neighbors related measures (nearest neighbor, first and second tier), while the spherical wavelet descriptors perform better than the lightfields descriptor for the precision/recall measures (DCG), which are considered more indicative.

An interesting result is that the performance on the DCG measure of the IWT_MOMENTS, a very compact descriptor, is almost similar to the LFD. A comparison with the performance of the EXT and H-EXT descriptors shows that moment-based wavelet descriptors (IWT_MOMENTS) have several benefits: (1) compactness, (2) rotation invariant without pose normalization, and (3) easy to compute.

Finally, note that our descriptors exhibit poor performance on the Nearest Neighbor measure compared to the LFD, GEDT, SHD and EXT, but outperforms H-EXT and D2. This may be justified by the fact that our parameterization takes only the extent of the shape in the radial direction, discarding interior details. We plan in the future to experiment with a combination of GEDT and wavelet descriptors.

6.2 Retrieval results

Finally, we executed series of shape matching experiments on the base test classification of the Princeton Shape Benchmark (PSB) [22]. We use the query set provided in the 3D Shape Retrieval Contest (SHREC3D). Recall that the queries are not part of the PSB. In all our experiments, we consider a retrieved model as relevant if it belongs to the same class as the query model.

Figure 5 shows the retrieval results for each of the four descriptors. By visually inspecting these results, we can see that the descriptors that use directly the wavelet coefficients perform better. This is predictable since the wavelet moments are very compact. An important point to outline is that the performance of SWT_MOMENTS is very poor compared to the other descriptors. This observation is further confirmed using performance measures (Table 1). This is because the size of the SWT_MOMENTS is very small compared to image wavelet moments since the number of decomposition levels is very small. Using more decomposition levels is computationally impractical when using the second generation wavelets.

7 Conclusions and future work

We proposed in this paper the use of the second generation wavelet analysis for 3D model retrieval. We showed that our new parameterization is more suitable for shape analysis as it is uniform and takes into account uniformly all the shape features. Then we proposed new shape descriptors based on the higher order statistical moments of the spherical wavelet sub-bands. These descriptors are compact and rotation invariant. Our results on the Princeton Shape Benchmark show that the new framework outperforms the spherical harmonic based descriptors in terms of Discount Cumulative Gain and precision-recall measures. An interesting property is that the moment descriptors, which are very compact, perform similarly to the LightField descriptor on the DCG measure when applied to EXT.

This work opens a number of issues that we would like to investigate in the future. First we found from our experiments that the developed descriptors behave poorly on stick like shapes. We believe that this is the drawback of the sampling procedure. Another issue is to experiment with different spherical wavelet basis and compare their performance on different classes of shapes. Finally, none of the developed descriptors perform equally in all situations and on all classes of

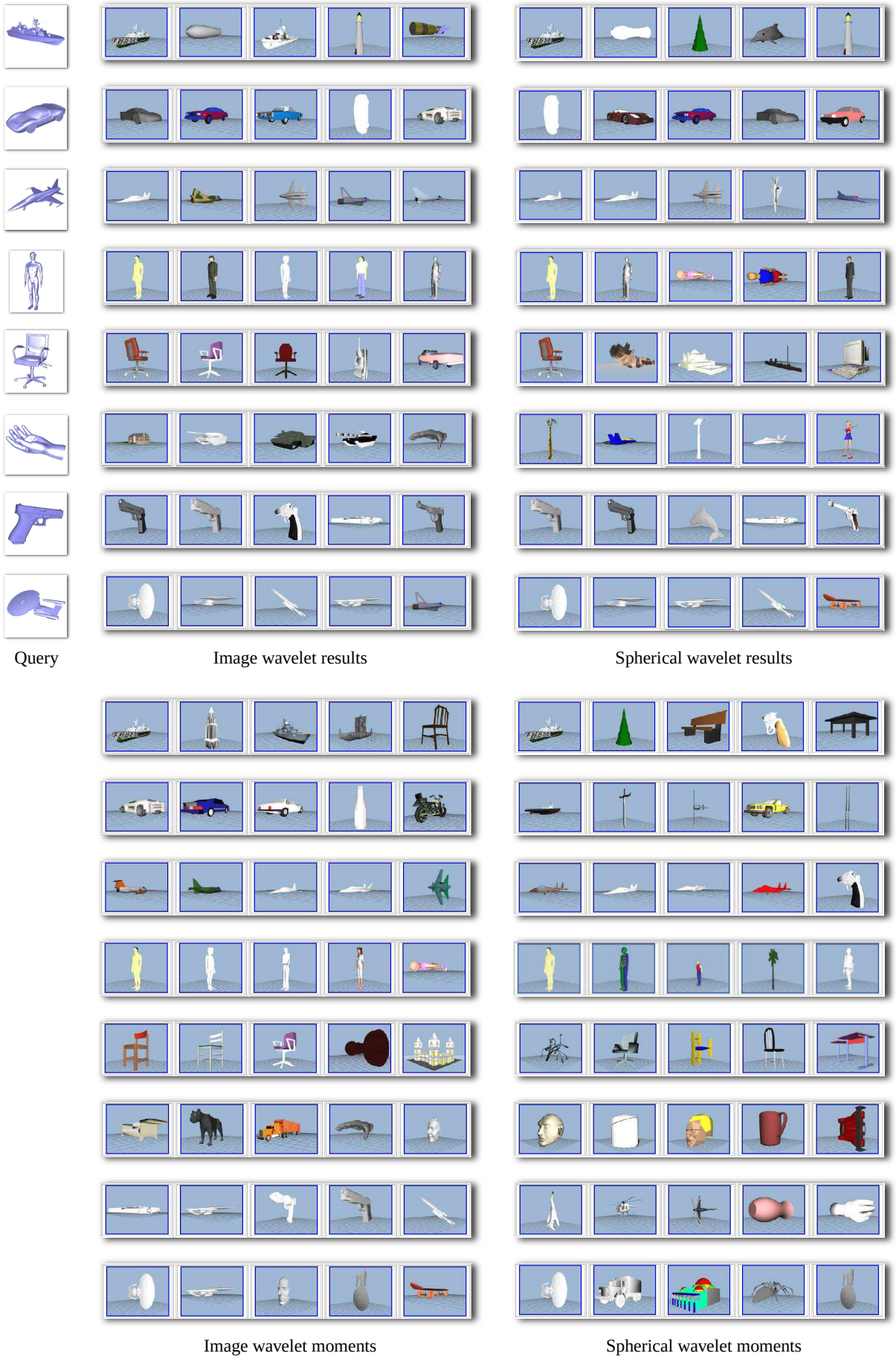

Fig. 5 Retrieval examples using random queries from the 3D Shape Retrieval Contest (SHREC3D). Recall that the queries are not part of the database.

shapes. A challenging issue is to investigate on how to combine and select features in order to achieve best performance.

References

1. Fast Spherical Wavelet Transform Package (FSWT). `http://www.ceremade.dauphine.fr/p̃eyre/`
2. Chen, D.Y., Tian, X.P., Shen, Y.T., Ouhyoung, M.: On visual similarity based 3d model retrieval. Computer Graphics Forum **22**(3), 223–232 (2003)
3. Cornea, N.D., Demirci, M.F., Silver, D., Shokoufandeh, A., Dickinson, S.J., Kantor, P.B.: 3d object retrieval using many-to-many matching of curve skeletons. In: SMI '05: Proceedings of the International Conference on Shape Modeling and Applications 2005 (SMI' 05), pp. 368–373. IEEE Computer Society, Washington, DC, USA (2005). DOI http://dx.doi.org/10.1109/SMI.2005.1
4. Do, M.N., Vetterli, M.: Texture similarity measurement using kullback-leibler distance on wavelet subbands. In: International Conference on Image Processing ICIP2000, pp. 730–733 (2000)
5. Do, M.N., Vetterli, M.: Wavelet-based texture retrieval using generalized gaussian density and kullback-leibler distance. IEEE Transactions on Image Processing **11**(2), 146–158 (2002)
6. Funkhouser, T.A., Min, P., Kazhdan, M.M., Chen, J., Halderman, J.A., Dobkin, D.P., Jacobs, D.P.: A search engine for 3d models. ACM Transactions on Graphics **22**(1), 83–105 (2003)
7. Hilaga, M., Shinagawa, Y., Kohmura, T., Kunii, T.L.: Topology matching for fully automatic similarity estimation of 3d shapes. In: Proceedings of the 28th annual conference on Computer graphics and interactive techniques, pp. 203–212. ACM Press (2001). DOI http://doi.acm.org/10.1145/383259.383282
8. Hoppe, H., Praun, E.: Shape compression using spherical geometry images. In: MINGLE 2003 Workshop. In Advances in Multiresolution for Geometric Modelling, N. Dodgson, M. Floater, M. Sabin (eds.), Springer-Verlag, 2, pp. 27–46 (2003)
9. Iyer, N., Jayanti, S., Lou, K., Kalyanaraman, Y., Ramani, K.: Three-dimensional shape searching: state-of-the-art review and future trends. Computer-Aided Design **37**(5), 509–530 (2005)
10. Johnson, A.: Spin-images: A representation for 3-d surface matching. Ph.D. thesis, Robotics Institute, Carnegie Mellon University, Pittsburgh, PA (1997)
11. Jolliffe, I.T.: Principal Component Analysis, 2nd edition edn. Springer (2002)
12. Kazhdan, M., Funkhouser, T., Rusinkiewicz, S.: Rotation invariant spherical harmonic representation of 3d shape descriptors. In: SGP '03: Proceedings of the 2003 Eurographics/ACM SIGGRAPH symposium on Geometry processing, pp. 156–164. Eurographics Association, Aire-la-Ville, Switzerland, Switzerland (2003)
13. Laga, H., Takahashi, H., Nakajima, M.: Spherical wavelet descriptors for content-based 3d model retrieval. In: SMI '06: Proceedings of the IEEE International Conference on Shape Modeling and Applications 2006 (SMI'06), pp. 75–85. IEEE Computer Society, Washington, DC, USA (2006). DOI http://dx.doi.org/10.1109/SMI.2006.39
14. Novotni, M., Klein, R.: 3d zernike descriptors for content based shape retrieval. In: SM '03: Proceedings of the eighth ACM symposium on Solid modeling and applications, pp. 216–225. ACM Press, New York, NY, USA (2003). DOI http://doi.acm.org/10.1145/781606.781639
15. Osada, R., Funkhouser, T., Chazelle, B., Dobkin, D.: Matching 3d models with shape distributions. In: Shape Modeling International, pp. 154–166. Genova, Italy (2001)
16. Paquet, E., Rioux, M., A.Murching, T.Naveen, A.Tabatabai: Description of shape information for 2-d and 3-d objects. Signal Processing: Image Communication **16**(1-2), 103–122 (2000)
17. Praun, E., Hoppe, H.: Spherical parametrization and remeshing. ACM Transactions on Graphics **22**(3), 340–349 (2003). DOI http://doi.acm.org/10.1145/882262.882274
18. Reuter, M., Wolter, F.E., Peinecke, N.: Laplace-beltrami spectra as "shape-dna" of surfaces and solids. Computer-Aided Design **38**(4), 342–366 (2006)
19. Sander, P.V., Wood, Z.J., Gortler, S.J., Snyder, J., Hoppe, H.: Multi-chart geometry images. In: SGP '03: Proceedings of the 2003 Eurographics/ACM SIGGRAPH symposium on Geometry processing, pp. 146–155. Eurographics Association, Aire-la-Ville, Switzerland, Switzerland (2003)
20. Saupe, D., Vranic, D.V.: 3d model retrieval with spherical harmonics and moments. In: B. Radig, S. Florczyk (eds.) DAGM-Symposium, *Lecture Notes in Computer Science*, vol. 2191, pp. 392–397. Springer (2001)
21. Schroder, P., Sweldens, W.: Spherical wavelets: efficiently representing functions on the sphere. In: SIGGRAPH '95: Proceedings of the 22nd annual conference on Computer graphics and interactive techniques, pp. 161–172. ACM Press (1995). DOI http://doi.acm.org/10.1145/218380.218439
22. Shilane, P., Min, P., Kazhdan, M., Funkhouser, T.: The princeton shape benchmark. In: SMI '04: Proceedings of the Shape Modeling International 2004 (SMI'04), pp. 167–178. IEEE Computer Society (2004). DOI http://dx.doi.org/10.1109/SMI.2004.63
23. Sundar, H., Silver, D., Gagvani, N., Dickinson, S.J.: Skeleton based shape matching and retrieval. In: Shape Modeling International, pp. 130–142 (2003)
24. Tangelder, J.W., Veltkamp, R.C.: A survey of content based 3d shape retrieval. In: Shape Modeling International 2004, Genova, Italy, pp. 145–156 (June 2004)
25. Vranic, D.V.: An improvement of rotation invariant 3d-shape based on functions on concentric spheres. In: ICIP2003, pp. 757–760 (2003)
26. V.Vranic, D.: 3d model retrieval. Phd dissertation, Universitat Leipzig, Institut Fur Informatik (2003)
27. van de Wouwer, G., Scheunders, P., van Dyck, D.: Statistical texture characterization from discrete wavelet representations. IEEE Transactions on Image Processing **8**(4), 592–598 (1999)